Glacial history of the Greenland Ice Sheet and a local ice cap in Qaanaaq, northwest Greenland

Anne Sofie Søndergaard[1], Nicolaj Krog Larsen[1,2], Jesper Olsen[3], Astrid Strunk[1], Sarah Woodroffe[4]

[1]Department of Geoscience, Aarhus University, Høegh Guldbergs Gade 2, 8000 Aarhus C, Denmark

[2] Centre for GeoGenetics, Natural History Museum of Denmark, University of Copenhagen, Øster Voldgade 5-7, 1350 Copenhagen K, Denmark

[3]Department of Physics and Astronomy, Aarhus University, Ny Munkegade 120, 8000 Aarhus C, Denmark

[4]Department of Geography, Durham University, Lower Mountjoy South Rd, Durham DH1 3LE, UK

Abstract

In this study, we present new information on the glacial history of the Greenland Ice Sheet (GrIS) and a local ice cap in Qaanaaq, northwest Greenland. We use geomorphological mapping, ^{10}Be exposure dating of boulders, analysis of lake cores, and ^{14}C dating of reworked marine molluscs and subfossil plants to constrain the glacial history. Our ^{14}C ages of reworked marine molluscs reveal that the ice extent in the area was at or behind its present-day position from 42.2±0.4 to 30.6±0.3k cal a BP after which the GrIS expanded to its maximum position during the Last Glacial Maximum. We find evidence of early ice retreat in the deep fjord (Inglefield Bredning) at 11.9±0.6 ka whereas the Taserssuit Valley was deglaciated ~4 ka later at 7.8±0.1k cal a BP. A proglacial lake record suggests that the local ice cap survived the Holocene Thermal Maximum but moss kill-dates reveal that it was smaller than present for a period of time before 3.3±0.1k until 0.9±0.1k cal a BP, following which the ice in the area expanded towards its Little Ice Age extent.

1. Introduction

Ice loss from Greenland, both from the melting of local glaciers and ice caps, as well as the Greenland Ice Sheet (GrIS), is one of the largest contributors to current global sea level rise (Meier et al., 2007). Recent observations show that the northwest Greenland ice margin is particularly vulnerable to climate change and is losing ice-mass faster than most other areas in Greenland (Kjeldsen et al., 2015; Khan et al., 2015; Kjær, 2012). It is therefore important to gain knowledge about the long term glacial history in northwest Greenland to determine its sensitivity to climate change (Lowell et al., 2013; Corbett et al., 2014).

During the Last Glacial Maximum (LGM), the GrIS covered the entire study area and extended all the way to the shelf edge in northwest Greenland where it coalesced with the Innuitian Ice Sheet (England, 1999; Blake et al., 1996; Funder et al., 2011; Georgiadis et al., 2018; Knudsen et al., 2008). The LGM ice cover of northwest Greenland was extensive, although the observed marine limits, which are lower than in many other parts of Greenland, point towards a less extensive and thinner ice sheet during the late Weichselian, c. 25-20 ka (Funder and Hansen, 1996; England et al., 2006). Following the termination of the LGM the GrIS began to retreat and became fully land-based in this region around 12-10k cal a BP (Funder et al., 2011; Corbett et al., 2014; Bennike and Björck, 2002).

Very little is known about Holocene ice fluctuations in northwest Greenland. However, recent results show that outlet glaciers close to Thule Air Base experienced a re-advance c. 9-8 ka (Corbett et al., 2014), which has though, been disputed by Farnsworth et al. (2018). Additionally, short term early Holocene cooling events around 9.3 ka and 8.2 ka has been observed further south around Disko Bay (Young et al., 2012) and on Baffin Island (Young et al., 2013; Axford et al., 2008). From subfossil plants incorporated into debris bands at the ice margin in Nunatarssuaq, Farnsworth et al. (2018) found that the GrIS extent in northwest Greenland was smaller than present at 4.7k cal a BP showing a response to the mid-Holocene warming and late Holocene cooling (Lecavalier et al., 2017; Lasher et al., 2017).

In this study, we constrain the local glaciation history of the GrIS and a local ice cap in the Qaanaaq area including Inglefield Bredning, northwest Greenland, using geomorphological mapping, ^{10}Be exposure dating of boulders on moraines and bedrock, analysis of lake sediment cores, and ^{14}C dating of reworked molluscs and subfossil plants. Furthermore, we assess the glacial history in the area with both local and regional climate records in order to expand our knowledge of

the long term local glacial history and constrain the sensitivity of the GrIS, its outlet glaciers and local ice caps to climate changes in northwest Greenland.

2. Geological Setting

The Qaanaaq area and Inglefield Bredning are situated in northwest Greenland around the town of Qaanaaq 77.4-77.7°N (Fig. 1). The Piulip Nunâ peninsula has a steep relief and a plateau at c. 600 m a.s.l. on which the Qaanaaq Ice Cap (QIC, informal name) is situated. The fjord of Inglefield Bredning, around 80 km in length, stretches from its head south of the Piulip Nunâ peninsula and into Murchison Sund. The Taserssuit Valley at the bottom of McCormick Fjord is c. 10 km long and has a characteristic u-shaped form and the valley floor is covered with glacial sediments and hosts several smaller lakes (Fig. 2). The valley is bound by the Piulip Nunâ peninsula and QIC to the south, McCormick Fjord to the west and glacier lobes from the GrIS flowing into the valley from north and east.

The bedrock in the area is mainly composed of Archean gneisses overlain by Late Proterozoic sedimentary and volcanic basin sediments from the Thule Supergroup (Henriksen et al., 2009; Dawes, 2006). In the Taserssuit Valley Quaternary sediments, mostly consisting of diamictic and fluvial material, cover the valley floor. The marine limit in the entire Thule region is not well constrained as only a few observations of marine bivalves from marine terraces have been made. At Qeqertat, in Inglefield Bredning, 75 km east-southeast of Qaanaaq, the marine limit is c. 73 m a.s.l. (Fredskild, 1985) and at Saunders Ø, close to Thule Air Base, c. 90 km south of Qaanaaq, the marine limit is c. 40 m a.s.l. (Funder, 1990).

3. Methods

3.1 Geomorphological mapping

Geomorphological mapping of the Taserssuit Valley was based on field observations, Landsat-8 images, air photographs taken during fieldwork in 2017 and the ArcticDEM explorer (Porter et al., 2018). Mapped landforms, as moraines, alluvial fans and lakes were ground-truthed in the field.

3.2 ^{14}C dating of reworked molluscs

In-situ marine molluscs collected from raised marine deposits can be used to set a minimum age constraint on the deglaciation of an area (Funder et al., 2011; Bennike and Björck, 2002) whereas marine molluscs reworked by advancing glaciers can be used to determine when the ice extent was smaller than present (Bennike and Weidick, 2001; Briner et al., 2014). In Taserssuit Valley, we collected reworked marine bivalve shells and shell fragments at four different sites (Fig. 2), ranging from 15 m a.s.l. to 52 m a.s.l, to determine when the valley potentially was ice-free and the ice extent smaller than today. The sample sites were chosen based on the presence of shell fragments and we did not find reworked molluscs further into the valley than our sample locations. From each sample site, three shell fragments were chosen, pre-treated following the procedure of (Brock et al., 2010), and ^{14}C dated at the Aarhus AMS Centre. Radiocarbon ages were calibrated using OxCal v4.3 (Ramsey, 2009) with the Marine13 calibration curve (Reimer et al., 2013) and a marine reservoir effect of 550 ^{14}C a (ΔR=150 ^{14}C a) based on a couple of ages from shells collected alive before 1960 in north Greenland (Mörner and Funder, 1990). Sample information, resulting ^{14}C ages, and calibrated ages are reported in Table 1. Throughout the text, we use the mean calibrated ^{14}C ages $\pm 2\sigma$.

3.3 ^{10}Be dating of boulders

Cosmogenic nuclide exposure dating can be used to constrain the deglaciation history for land areas during glacial times (Gosse and Phillips, 2001; Ivy-Ochs and Kober, 2008). In this study, we used ^{10}Be exposure dating of boulders to determine the age of two moraine systems in the Taserssuit Valley (Fig. 2), most likely deposited by outlet glaciers, as well as the timing of the deglaciation of an island in Inglefield Bredning (Fig. 1).

Using a rock saw, hammer and chisel we cut rock samples from the top few centimeters of individual quartz bearing stable boulders. With a hand-held Garmin e-trex 30 GPS, we recorded the latitude, longitude and elevation of each sample. The orientation of the rock surface and shielding by the surrounding topography were measured using a compass and clinometer, respectively. Elevations of boulders chosen for sampling were all between 74 m a.s.l. and 128 m a.s.l., and thus, were all collected above the assumed marine limit of the area (Lecavalier et al., 2014; Fredskild, 1985; Funder, 1990). We measured sample thicknesses with a caliper before crushing and sieving the samples to 250-700 μm. From this fraction we isolated quartz, and extracted beryllium.

The ^{10}Be samples were processed in the Cosmogenic Nuclide Laboratory at Department of Geoscience, Aarhus University following methods modified from (Corbett et al., 2016). Sample ^{10}Be/^{9}Be ratios were measured at the Aarhus AMS Centre. We calculated ^{10}Be ages (Table 2) using the online exposure age calculator formerly known as the CRONUS-Earth online exposure calculator v.3 (Balco et al., 2008), the Baffin Bay/Arctic production rate (Young et al., 2013), and the St production scaling scheme (Lal, 1991; Stone, 2000) as the effect from changes in the geomagnetic field over time is minimal at high latitudes. All variables used in the calculations can be seen in Table 2. The density of 2.65 g/m^3 were chosen as it is representative for the boulders we sampled and we assumed zero erosion. We have not made any corrections for cover by vegetation or snow as the vegetation in the area is sparse and boulders sampled were all in open elevated locations in the landscape making it highly likely that any snow covering the boulders will have persisted for only a short period of time. ^{10}Be age results are presented with 1σ internal uncertainty and ages calculated using other scaling schemes deviate by <1%.

3.4 Analysis of lake sediment cores

Proglacial lake records can be used to determine ice marginal fluctuations as the ice marginal position relative to the lake catchment influences the sediments deposited in the lake (Briner et al., 2011; Larsen et al., 2011). In addition, basal ages from lake records can be used to constrain a minimum timing of the formation of the lakes and thus, the deglaciation of an area. In this study we target 5 lakes in total, one proglacial lake and four smaller lakes, none of which are proglacial. The Taserssuit proglacial lake that still receives glacial meltwater, referred to as Q3 in this study (Fig. 2), is used to constrain ice marginal fluctuations of the local outlet glaciers from the GrIS and QIC in the Qaanaaq area. In addition, we determine the timing of deglaciation of Taserssuit Valley based on ^{14}C dating of basal sediments from four smaller lakes, Q4, Q5a, Q6 and Q7 (Fig. 2).

All lakes were cored using a tapper corer as close to the center of the lakes as possible. The water depths at the coring places were measured using a handheld echo sounder type Plastimo Echotest II and the retrieved sediment cores had lengths between 22 cm and 145 cm. The chosen lakes were at different elevations ranging from 16 m a.s.l. to 79 m a.s.l. with only Q7 being above the assumed marine limit of the Thule region (Lecavalier et al., 2014; Fredskild, 1985; Funder, 1990). After retrieving the cores, they were drained to remove leftover water and stabilized before

they were packed and transported to Denmark where they were stored at 2-4°C. All cores were photographed and XRF scanned at 2 mm resolution using an Itrax core scanner at the Department of Geoscience, Aarhus University. Magnetic susceptibility was measured at 0.5 cm resolution using a Bartington instrument. The cores were described in terms of lithology. Samples for diatom and foraminiferal analysis were taken as close to the base as possible at centimeter intervals with 5 samples collected in sediment core Q4 and only one sample in core Q3, Q5a, Q6 and Q7 respectively, with Q5a and Q7 being basal samples. Macrofossils at the bottom of each core were sampled for ^{14}C dating. Bulk sediment samples were used where we were unable to find sufficient macrofossils for dating. Both macrofossil and bulk samples were sent to the Aarhus AMS Centre for pre-treatment and ^{14}C dating following the procedure from Brock et al. (2010). Radiocarbon ages were calibrated using OxCal v4.3, with the IntCal 13 calibration curve (Reimer et al., 2013) and are reported in Table 1. Throughout the text, we use the mean calibrated ^{14}C ages $\pm 2\sigma$.

3.5 ^{14}C dating of subfossil plants

Radiocarbon dating of subfossil plants obtained in front of a melting glacier can be used to constrain the onset of ice cap growth beyond its present-day ice margin and thus constrain a time when the ice cap was smaller than today (Lowell et al., 2013; Miller et al., 2012). In this study, we collected and dated subfossil plants which have recently been exposed by QIC margin recession. The sub-fossil plants were sampled in-situ at varying distances from the ice cap. On the southern side of the ice cap, all samples were collected within a distance of 30 centimeters from the ice cap margin, whereas the samples on the northern side were collected between 20 cm and 25 m from the ice cap margin. We were aware of the risk of contamination by growth of new plants (Miller et al., 2012) and thus, only collected samples in areas without modern growth. Furthermore, we only collected mosses rooted into the soil to make sure that they were growing in-situ. In total, we collected three samples from the southern side of the ice cap margin (MC11-13) and eight samples from the northern side of the ice cap margin (MC2-9) (Fig. 1). All samples were rinsed and subsequently sent to Aarhus AMS Centre for pre-treatment and ^{14}C dating. Radiocarbon ages were calibrated using OxCal v4.3 with the IntCal13 calibration curve (Reimer et al., 2013) and are reported in Table 1. Throughout the text, we use the mean calibrated ^{14}C ages $\pm 2\sigma$.

4. Results, description and interpretation

4.1 Geomorphological mapping

A geomorphological map of the Taserssuit Valley was constructed (Fig. 2). The valley bottom rises from 5 m a.s.l. in the western part of the area up to ~45 m a.s.l. in the eastern part of the area. Both the northern and southern boundaries of the valley rise up to above 600 m a.s.l. with the plateau on the southern side being partly covered by the QIC.

From the plateau on the northern side, alluvial fans stretch out towards the valley bottom. Meltwater streams from the ice on both plateaus run down towards the valley bottom. The valley floor is covered with numerous lakes of varying size. One larger lake, Q3, is situated in the center of the valley at about 16 m a.s.l., three smaller lakes, Q4, Q5a and Q6, in the northwestern part of the valley is at approximately 40 m a.s.l., and several smaller lakes, including Q7, are located in the southeastern part of the valley, located up to ~80 m a.s.l.

The southern part of the valley floor is characterized by a gently hummocky terrain with smaller hills and depressions, most likely created by slow ice retreat and stagnant ice being left in the valley after the deglaciation. The surface is in most areas covered by diamictic material and fluvial sediments. Two sets of moraine systems have been identified in the Taserssuit Valley. One system, an ice-proximal, fresh-looking, high crested set of moraines with little or no vegetation and unconsolidated diamictic sediments are visible in the southern and eastern part of the valley and are created by ice lobes emerging from the northern side of the QIC and outlet glaciers from the GrIS. The other system, consisting of fairly distinct weathered moraines, further away from the ice margin is visible in the landscape in the northeastern and southwestern parts of the valley. These older moraines have a less steep relief, little vegetation and consist of more firm sediments.

4.2 ^{14}C dating of reworked shells

Reworked marine molluscs and mollusc fragments were collected from four different sites in the Taserssuit Valley, a total of 12 samples, 3 from each site (Fig. 2). The molluscs were found on the sediment surface and within diamictic sediments at different elevations ranging from 14 to 52 m a.s.l. Several species were identified but only *Hiatella arctica* and *Mya truncata* were used for ^{14}C

dating. The calibrated mean ^{14}C ages range from 30.6k cal a BP (Q-S3c) to 42.2k cal a BP (Q-S3b), with all but one being older than 34k cal a BP (Table 1).

We interpret the molluscs to have been re-deposited and thus, the ages of the molluscs to constrain a time where the ice in the area were behind its present day extent.

4.3 ^{10}Be dating of boulders

A total of five boulders for ^{10}Be exposure dating were sampled in the Taserssuit Valley, two boulders (GL1739 and GL1740) on top of a moraine in the eastern part of the valley and three boulders (GL1736, GL1737 and L1738) on top of a moraine in the western part of the valley (Fig. 2 and Fig. 3). The measured ^{10}Be concentrations in the five boulder samples resulted in exposure ages ranging from 10.4±0.6 to 28.6±0.9 ka with no clear distribution or clustering even when uncertainties are considered (Fig. 3, Table 2, Fig. S1). GL1740 resulted in the oldest boulder age of 28.6±0.9 ka and is from a boulder on top of the moraine in the eastern part of the valley whereas GL1736, from a boulder on top of the moraine in the western part of the valley, yielded the youngest boulder age of 10.4±0.6 ka. It is not possible to calculate a mean age for the five boulders as none of the ^{10}Be ages from the two moraines overlap within 2σ.

The five boulders collected in the Tassersuit Valley are most likely affected by inheritance which would explain the large range in ages and thus, cannot be used to constrain ice fluctuations in the valley.

Additionally, three boulders on bedrock (GL1742-1744) were sampled on an island at the head of Inglefield Bredning (Fig. 1 and 3). The measured ^{10}Be concentrations in these boulder samples resulted in exposure ages ranging from 10.9±0.5 to 13.1±0.6 ka (Fig. 3, Table 2 and Fig. S1) overlapping within 2σ, resulting in an average of 11.9±0.6 ka which we interpret as a maximum constrain on the deglaciation of the inner part of Inglefield Bredning.

4.4 Analysis of lake sediment cores

The sediment record from the proglacial lake (Q3) is 59 cm long and consists of laminated silty-clay (Fig. 4). The sediment is red and orange at the top (0-12 cm) with a transition zone towards more light brown sediment colors in the middle (12-24 cm) and only light brown colors from 24 cm

to the bottom. We were unable to find any macrofossils in the core and a bulk sample at 58-59 cm depth was used for ^{14}C dating yielding an age of 7.2±0.2k cal a BP (Fig. 4 and Table 1).

We interpret that the lake continued to receive meltwater from its formation 7.2±0.2k cal a BP until present based on the lack of organic-rich gyttja and the fact that there are no significant lithological or geochemical changes in the sediment core. Accordingly, both QIC and outlet glaciers from the GrIS most likely remained in its catchment throughout the Holocene.

Basal ^{14}C ages from the four other lake records, Q4, Q5a, Q6 and Q7, were used to set a minimum constrain on the timing of the formation of the lakes and thus, the deglaciation of the Taserssuit Valley. Cores Q4, Q5a and Q7 are between 111 and 158 cm long. All three consist of slightly laminated clay-gyttja, with mm-to-cm thick bands of organic material which become more frequent toward the bottom (Fig. 4). In all three cores, the sediment has a red and orange color at the top with a transition to a greyer color towards the bottom. Sediment samples were analyzed for foraminifera and diatom assemblages. No foraminifera were found within the basal sediments of the cores and the main diatom species found were *Fragilariforma virescens, Amphora ovalis, Tabellaria flocculosa,* and *Fragilaria construens*, which are all freshwater species. Macrofossils were retrieved in core Q4, Q5a, and Q7 with resulting basal ^{14}C ages of 7.8±0.1k cal a BP, 5.4±0.2k cal a BP, 7.0±0.1k cal a BP respectively (Fig. 4 and Table 1). Core Q6 is short, 22 cm, and has light-brown sandy sediment at the top (0-11 cm). The rest of the core is silty-clay with a dark-brown color. No macrofossils were present, so a bulk sample was collected for ^{14}C dating. The bulk sample from core Q6, retrieved at 9.5-10.5 cm depth resulted in an age of 1.5±0.1k cal a BP (Fig. 4 and Table 1).

We interpret the oldest basal age of c. 7.8±0.1k cal a BP from core Q4 as a minimum age of the local deglaciation of the Taserssuit Valley. There is no clear pattern in the age distribution related to stratigraphy, elevation or location in the valley. We find no evidence of marine deposition in any of the sediment cores even at low elevation and this, together with the lack of postglacial marine molluscs, suggests that the valley floor was not inundated by the sea at any time during the Holocene.

4.5 ^{14}C dating of subfossil plants

A total of 11 moss samples were collected in front of the QIC, eight from the northern side of the ice cap and three from the southern side of the ice cap. Resulting ages of the moss samples group within two different time intervals. All eight moss samples (MC2-MC9) from the northern side of the QIC range in age from 0.9±0.1 to 1.2±0.1k cal a BP and the three moss samples (MC11-MC13) from the southern side range in age from 3.1±0.1 to 3.3±0.1k cal a BP (Fig. 5, Table 1 and Fig. S2). There is no clear correlation between the distance from the sampling site to the present day ice cap margin and the resulting ^{14}C ages, even though samples were collected up to a distance of 25 metres from the ice cap margin, showing that contamination was not an issue.

We interpret the ages as constraining a time of ice cap growth beyond its present day extent and thus, suggest that by 3.3±0.1k and 0.9±0.1k cal a BP, the ice cap were beyond its present day extent in both the northern and southern part respectively.

5. Discussion

5.1 MIS 3 and LGM glacial history

The age distribution of reworked molluscs show that the Taserssuit Valley was ice-free during Marine Isotope Stage 3 (MIS 3) between 42.2±0.4 and 30.6±0.3k cal a BP and that the GrIS extent was similar or even smaller than today (Fig. 6). Furthermore, the age distribution of molluscs indicates that the GrIS began its expansion towards the LGM extent after c. 30.6±0.3k cal a BP. On Ellesmere Island and from the Carey Islands radiocarbon dating of reworked shell fragments in sediments gave similar ages between 50.6 and 31.9k cal a BP (Blake, 1992) suggesting that the expansion of the Innuitian Ice Sheet and coalescence with the GrIS occurred after c. 30k cal a BP and maybe as late as c. 22k cal a BP (England, 1999). However, it should be noted that many of the existing dates are conventional radiocarbon ages of several molluscs and should be treated with caution. In northeast Greenland, a recent study based on dating of reworked mollusc fragments in moraines reached a similar conclusion that the GrIS was smaller than present during MIS 3 (41-26k cal a BP) and that the LGM expansion occurred after 26k cal a BP (Larsen et al., 2018). Overall, these findings suggest that the GrIS extent in northern Greenland was similar to today or even smaller during MIS 3. A possible explanation for the limited MIS 3 ice extent could be a combination of relative warm summer temperatures, ~6-8°C warmer than LGM because of higher

boreal summer insolation, and low snow accumulation rates (Larsen et al., 2018; Buizert et al., 2014).

5.2 Holocene glacial history

The oldest basal ^{14}C age from the lake sediment cores indicate that the deglaciation of the Taserssuit Valley occurred around 7.8±0.1k cal a BP. As the ^{10}Be ages of boulders sampled in the Taserssuit Valley gave a large spread of ages from 10.4±0.6 to 28.6±0.9 ka this suggests, together with the oldest lake sediment ^{14}C age, that the boulders are most likely affected by inheritance and point toward generally low erosion rates in the area. Accordingly, it is meaningless to calculate a mean of the ^{10}Be ages from the two moraines. However, the timing of moraine formation is most likely closest to but still younger than the youngest ^{10}Be age of 10.4±0.6 ka. The younger moraines in the study area have been created from advancing glaciers from the GrIS and QIC but whether the older set of moraines have been created by an ice still stand during deglaciation or by an ice re-advance in early Holocene is not possible to constrain. Recent studies from the Thule area faced similar problems with inheritance in boulder samples and it was concluded that the ice in the area was most likely cold based and thus, less erosive (Corbett et al., 2014; Farnsworth et al., 2018).

The apparent old ages from the marine molluscs, the relatively young basal ages from the lakes and the lack of marine material in the sediment cores suggest that the Taserssuit Valley was ice-covered during early Holocene until c. 7.8±0.1k cal a BP (Fig. 6), most likely by a slow retreating ice covering the valley joining what is now the GrIS and QIC. This is surprising as our new ^{10}Be ages from Inglefield Bredning suggest deglaciation of the fjord between 13.1±0.6 and 10.9±0.5 ka, with an average of 11.9±0.6 ka which is in accordance with earlier findings showing that the deglaciation of Inglefield Bredning occurred around 10.2k cal a BP with the inner part of a small side fjord being ice free by 9.6k cal a BP (Bennike and Björck, 2002). Summer temperatures as much as 2.5-4 °C higher than today have been inferred from a lake about 100 km south of Taserssuit Valley close to Thule Air Base in northwest Greenland, suggesting a relatively warm early and middle Holocene (Lasher et al., 2017) which supports the early deglaciation of the area.

However, ice often retreats faster in deep fjords compared to shallow fjords or on land (England, 1999; Batchelor et al., 2018; Larsen et al., 2014) and this may explain why the ice retreat in the relatively low relief Taserssuit Valley was slower and led to a later deglaciation compared to

the adjacent Olrik fjord, Inglefield Bredning and Wolstenholme Fjord which were deglaciated already in the Early Holocene (Corbett et al., 2014; Fredskild, 1985; Bennike and Björck, 2002).

Since the deglaciation of the Taserssuit Valley, the proglacial lake Q3 has received glacial meltwater continuously until today. This could suggest that neither the GrIS or QIC completely retreated out of the catchment of lake Q3 and thus, most likely survived the warm Holocene Thermal Maximum in accordance with the overall trend for local glaciers and ice caps in North Greenland (Larsen et al., 2019). We can though, not distinguish if the sediment in core Q3 originates from the GrIS or QIC or both, but we do expect QIC to have had similar behavior to climate fluctuations as the outlet glaciers from the GrIS since its possible re-initiation in middle Holocene. The radiocarbon ages of moss samples demonstrate that the QIC was smaller than its present day extent a period of time until between 3.3±0.1 and 0.9±0.1k cal a BP (Fig. 6), with a complete re-advance of the entire ice cap after 0.9±0.1k cal a BP, which correlates well with atmospheric temperature records from the area, pointing towards the coldest period during the Holocene to be after 1.2 ka (Lasher et al., 2017). Clear fresh looking trimlines and eroded surfaces in the landscape in front of QIC, both on the northern and southern side (Fig. 5), as well as young distinct moraines made by ice lobes from QIC and the GrIS (Fig. 2), mark the presumed Little Ice Age extent of the ice in the study area. We have not been able to constrain the timing of its initiation but can conclude that a re-advance initiated at or possibly before 3.3±0.1k cal a BP lasting until the glaciers and ice cap reached their Little Ice Age extent. Since then, QIC, its ice lobes and outlet glaciers from the GrIS have all been retreating in the Qaanaaq area.

6. Conclusion

Our results show that the Taserssuit Valley was ice free from 42.2±0.4 to 30.6±0.3k cal a BP, which is in accordance with a late LGM ice buildup in northwest Greenland. This suggests that the GrIS was similar in size to today or even smaller during MIS 3 possibly because of its sensitivity to relatively high summer air temperatures and low snow accumulation rates. Following the LGM the GrIS began to retreat from its maximum position and it reached the present coast line by 11.9±0.6k cal a BP. The ice retreat occurred faster in the deep and wide Inglefield Bredning compared to the peninsulas and land areas of the surrounding coast. Thus, the Taserssuit Valley was possibly occupied with a slow retreating ice until the early Holocene, connecting what is now the QIC with the GrIS and preventing marine inundation of the Taserssuit Valley. By 7.8±0.1k cal a BP the

Taserssuit Valley was deglaciated and the QIC was separated from the GrIS. The outer moraine system present in the valley could be evidence of a possible still stand or re-advance during the early Holocene. However, the large scatter in the ^{10}Be ages ranging from 10.4±0.6 to 28.8±0.9 ka, probably because of nuclide inheritance, makes it impossible to make any firm conclusions. After the initial deglaciation of the valley, the ice retreated behind its present day extent. At 3.3±0.1k cal a BP, or possibly before, the ice started re-advancing and was at or more extensive than its present day extent at 0.9±0.1k cal a BP. The ice further advanced towards its presumed Little Ice Age maximum extent, leaving clear trimlines, eroded surfaces and moraines in the landscape. The dynamic glacial history in the Qaanaaq area and Inglefield Bredning shows a distinct correlation to atmospheric temperature fluctuations known to have happened in northwest Greenland. It clearly shows that the GrIS is sensitive to temperature fluctuations and changes in precipitation and also highlights the importance of fjord bathymetry in relation to ice retreat rates. On smaller scale, local ice caps and outlet glaciers seem to have a great sensitivity to temperature fluctuations as well, being especially well constrained in late Holocene. Overall, these new findings strengthen our knowledge about the sensitivity of ice sheets as well as more local ice caps and glaciers to climate fluctuations, especially sensitivity to a warmer climate, helping improve models and predictions of future contributions to sea level rise from both the GrIS and local glaciers and ice caps.

Acknowledgement

This research was supported by Aarhus University Research Foundation, Aarhus University Arctic Research Centre, and the Villum Foundation. We thank Thomas A. Davidson, Jari Syväranta, Torben L. Lauridsen, Mikkel F. Schou and Sveinn Brynjólfsson for support during fieldwork as well as Svend Funder for identifying the molluscs used for radiocarbon dating and Bent Odgaard for identifying macrofossils used for radiocarbon dating. Birte Lindahl Eriksen, Rikke Brok Jensen and Marianne Lyngholm Nielsen are thanked for help with laboratory work. We thank Lena Håkansson and two anonymous reviewers for constructive comments and sugestions for changes relating to a previous version of this manuscript.

Supporting Information

Figure S1. Kernel density plots for West Taserssuit Moraine (GL1736, GL1737 and GL1738), East Taserssuit Moraine (GL1739 and GL1740) and Inglefield Bredning (GL1742, GL1743 and GL1744).

Figure S2. Probability plots for calibrated ^{14}C ages of subfossil plants collected at the ice margin on the northern (MC2-MC9) and southern (MC11-MC13) side of Qaanaaq Ice Cap.

References

Axford, Y.,Briner, J. P.,Miller, G. H. & Francis, D. R. 2008. Paleoecological evidence for abrupt cold reversals during peak Holocene warmth on Baffin Island, Arctic Canada. *Quaternary Research,* 71**,** 142-149.

Balco, G.,Stone, J. O.,Lifton, N. A. & Dunai, T. J. 2008. A complete and easily accessible means of calculating surface exposure ages or erosion rates from 10Be and 26Al measurements. *Quaternary Geochronology,* 3**,** 174-195.

Batchelor, C. L.,Dowdeswell, J. A. & Rignot, E. 2018. Submarine landforms reveal varying rates and styles of deglaciation in North-West Greenland fjords. *Marine Geology,* 402**,** 60-80.

Bennike, O. & Björck, S. 2002. Chronology of the last recession of the Greenland Ice Sheet. *Journal of Quaternary Science,* 17**,** 211-219.

Bennike, O. & Weidick, A. 2001. Late Quaternary history around Nioghalvfjerdsfjorden and Jøkelbugten, North-East Greenland. *Boreas,* 30**,** 205-227.

Blake, W. 1992. Shell-bearing till along Smith Sound, Ellesmere Island - Greenland: age and significance. *Sveriges Geologiska Undersokning***,** 51-58.

Blake, W.,Jackson, H. R. & Currie, C. G. 1996. Seafloor evidence for glaciation, northernmost Baffin Bay. *Bulletin og the Geological Society of Denmark,* 43**,** 157-168.

Briner, J. P.,Kaufman, D. S.,Bennike, O. & Kosnik, M. A. 2014. Amino acid ratios in reworked marine bivalve shells constrain Greenland Ice Sheet history during the Holocene. *Geology,* 42**,** 75-78.

Briner, J. P.,Young, N. E.,Thomas, E. K.,Stewart, H. a. M.,Losee, S. & Truex, S. 2011. Varve and radiocarbon dating support the rapid advance of Jakobshavn Isbræ during the Little Ice Age. *Quaternary Science Reviews,* 30**,** 2476-2486.

Brock, F.,Higham, T.,Ditchfield, P. & Ramsey, C. B. 2010. Current Pretreatment Methods for AMS Radiocarbon Dating at the Oxford Radiocarbon Accelerator Unit (Orau). *Radiocarbon,* 52**,** 103-112.

Buizert, C.,Gkinis, V.,Severinghaus, J. P.,He, F.,Lecavalier, B. S.,Kindler, P.,Leuenberger, M.,Carlson, A. E.,Vinther, B.,Masson-Delmotte, V.,White, J. W. C.,Liu, Z.,Otto-Bliesner, B. & Brook, E. J. 2014. Greenland temperature response to climate forcing during the last deglaciation. *Science,* 345**,** 1177-1180.

Corbett, L. B.,Bierman, P. R.,Lasher, G. E. & Rood, D. H. 2014. Landscape chronology and glacial history in Thule, northwest Greenland. *Quaternary Science Reviews,* 109**,** 57-67.

Corbett, L. B.,Bierman, P. R. & Rood, D. H. 2016. An approach for optimizing in situ cosmogenic 10 Be sample preparation. *Quaternary Geochronology,* 33**,** 24-34.

Dawes, P. R. 2006. Explanatory notes to the geological map of Greenland, 1:500 000.

England, J. 1999. Coalescent Greenland and Innuitian ice during the Last Glacial Maximum: revising the Quaternary of the Canadian High Arctic. *Quaternary Science Reviews,* 18**,** 421-46.

England, J.,Atkinson, N.,Bednarski, J.,Dyke, A. S.,Hodgson, D. A. & Ó Cofaigh, C. 2006. The Innuitian Ice Sheet: configuration, dynamics and chronology. *Quaternary Science Reviews,* 25**,** 689-703.

Farnsworth, L. B.,Kelly, M. A.,Bromley, G. R. M.,Axford, Y.,Osterberg, E. C.,Howley, J. A.,Jackson, M. S. & Zimmerman, S. R. 2018. Holocene history of the Greenland Ice-Sheet margin in Northern Nunatarssuaq, Northwest Greenland. *arktos,* 4.

Fredskild, B. 1985. The Holocene vegetational development of Tugtuligssuaq and Qeqertat, Northwest Greenland. *Meddelelser om Grønland, Geoscience,* 14.

Funder, S. 1990. Late Quaternary stratigraphy and glaciology in the Thule area, northwest Greenland. *Meddelelser om Grønland,* 22.

Funder, S. & Hansen, L. 1996. The Greenland ice sheet - a model for its culmination and decay during and after the last glacial maximum. *42*.

Funder, S.,Kjeldsen, K. K.,Kjær, K. H. & Ó Cofaigh, C. 2011. The Greenland Ice Sheet During the Past 300,000 Years: A Review. 15**,** 699-713.

Georgiadis, E.,Giraudeau, J.,Martinez, P.,Lajeunesse, P.,St-Onge, G.,Schmidt, S. & Massé, G. 2018. Deglacial to postglacial history of Nares Strait, Northwest Greenland: a marine perspective. *Climate of the Past Discussions***,** 1-29.

Gosse, J. C. & Phillips, F. M. 2001. Terrestrial in situ cosmogenic nuclides: theory and application. *Quaternary Science Reviews,* 20**,** 1475-1560.

Henriksen, N.,Higgins, A. K.,Kalsbeek, F. & Pulvertaft, T. C. R. 2009. Greenland from archean to quaternary: Descriptive text to the 1995 geological map of greenland, 1:2 500 000. *Geological Survey of Denmark and Greenland Bulletin* 18.

Ivy-Ochs, S. & Kober, F. 2008. Surface exposure dating with cosmogenic nuclides. *Quaternary Science Journal,* 57**,** 179-209.

Khan, S. A.,Aschwanden, A.,Bjork, A. A.,Wahr, J.,Kjeldsen, K. K. & Kjaer, K. H. 2015. Greenland ice sheet mass balance: a review. *Rep Prog Phys,* 78**,** 046801.

Kjær, K. H., Khan, S. A., Korsgaard, N. J., Wahr, J., Bamber, J. L., Hurkmans, R., Van Den Broeke, M., Timm, L. H., Kjeldsen, K. K., Bjørk, A. A., Larsen, N. K., Jørgensen, L. T., Færch-Jensen, A., Willerslev, E. 2012. Aerial Photographs Reveal Late-20th-Century Dynamic Ice Loss in Northwestern Greenland. *Science,* 337**,** 569-573.

Kjeldsen, K. K.,Korsgaard, N. J.,Bjork, A. A.,Khan, S. A.,Box, J. E.,Funder, S.,Larsen, N. K.,Bamber, J. L.,Colgan, W.,Van Den Broeke, M.,Siggaard-Andersen, M. L.,Nuth, C.,Schomacker, A.,Andresen, C. S.,Willerslev, E. & Kjaer, K. H. 2015. Spatial and temporal distribution of mass loss from the Greenland Ice Sheet since AD 1900. *Nature,* 528**,** 396-400.

Knudsen, K. L.,Stabell, B.,Seidenkrantz, M.-S.,Eiríksson, J. & Blake, W. 2008. Deglacial and Holocene conditions in northernmost Baffin Bay: sediments, foraminifera, diatoms and stable isotopes. *Boreas,* 37**,** 346-376.

Lal, D. 1991. Cosmic ray labeling of erosion surface: in situ nuclide production rates and erosion models. *Earth and Planetary Science Letters,* 104**,** 424-439.

Larsen, N. K.,Funder, S.,Kjær, K. H.,Kjeldsen, K. K.,Knudsen, M. F. & Linge, H. 2014. Rapid early Holocene ice retreat in West Greenland. *Quaternary Science Reviews,* 92**,** 310-323.

Larsen, N. K.,Kjær, K. H.,Olsen, J.,Funder, S.,Kjeldsen, K. K. & Nørgaard-Pedersen, N. 2011. Restricted impact of Holocene climate variations on the southern Greenland Ice Sheet. *Quaternary Science Reviews,* 30**,** 3171-3180.

Larsen, N. K.,Levy, L. B.,Carlson, A. E.,Buizert, C.,Olsen, J.,Strunk, A.,Bjork, A. A. & Skov, D. S. 2018. Instability of the Northeast Greenland Ice Stream over the last 45,000 years. *Nat Commun,* 9**,** 1872.

Larsen, N. K.,Levy, L. B.,Strunk, A.,Søndergaard, A. S.,Olsen, J. & Lauridsen, T. L. 2019. Local ice caps in Finderup Land, North Greenland, survived the Holocene Thermal Maximum. *Boreas*.

Lasher, G. E.,Axford, Y.,Mcfarlin, J. M.,Kelly, M. A.,Osterberg, E. C. & Berkelhammer, M. B. 2017. Holocene temperatures and isotopes of precipitation in Northwest Greenland recorded in lacustrine organic materials. *Quaternary Science Reviews,* 170**,** 45-55.

Lecavalier, B. S.,Fisher, D. A.,Milne, G. A.,Vinther, B. M.,Tarasov, L.,Huybrechts, P.,Lacelle, D.,Main, B.,Zheng, J.,Bourgeois, J. & Dyke, A. S. 2017. High Arctic Holocene temperature record from the Agassiz ice cap and Greenland ice sheet evolution. *Proc Natl Acad Sci U S A.*

Lecavalier, B. S.,Milne, G. A.,Simpson, M. J. R.,Wake, L.,Huybrechts, P.,Tarasov, L.,Kjeldsen, K. K.,Funder, S.,Long, A. J.,Woodroffe, S.,Dyke, A. S. & Larsen, N. K. 2014. A model of Greenland ice sheet deglaciation constrained by observations of relative sea level and ice extent. *Quaternary Science Reviews,* 102**,** 54-84.

Lowell, T. V.,Hall, B. L.,Kelly, M. A.,Bennike, O.,Lusas, A. R.,Honsaker, W.,Smith, C. A.,Levy, L. B.,Travis, S. & Denton, G. H. 2013. Late Holocene expansion of Istorvet ice cap, Liverpool Land, east Greenland. *Quaternary Science Reviews,* 63**,** 128-140.

Meier, M. F.,Dyurgerov, M. B.,Rick, U. K.,O'neel, S.,Pfeffer, W. T.,Anderson, R. S.,Anderson, S. P. & Glazovsky, A. F. 2007. Glaciers Dominate Eustatic Sea-Level Rise in the 21st Century. *Science,* 317**,** 1064-1067.

Miller, G. H.,Geirsdóttir, Á.,Zhong, Y.,Larsen, D. J.,Otto-Bliesner, B. L.,Holland, M. M.,Bailey, D. A.,Refsnider, K. A.,Lehman, S. J.,Southon, J. R.,Anderson, C.,Björnsson, H. & Thordarson, T. 2012. Abrupt onset of the Little Ice Age triggered by volcanism and sustained by sea-ice/ocean feedbacks. *Geophysical Research Letters,* 39**,** n/a-n/a.

Mörner, N. A. & Funder, S. V. 1990. C-14 dating of samples collected during the NORDQUA 86 expedition, and notes on the marine reservoir effect. *Meddelelser om Grønland,* 22**,** 57-59.

Nishiizumi, K.,Imamura, M.,Caffee, M. W.,Southon, J. R.,Finkel, R. C. & Mcaninch, J. 2007. Absolute calibration of 10Be AMS standards. *Nuclear Instruments and Methods in Physics Research Section B: Beam Interactions with Materials and Atoms,* 258**,** 403-413.

Porter, C.,Morin, P.,Howat, I.,Noh, M.-J.,Bates, B.,Peterman, K.,Keesey, S.,Schlenk, M.,Gardiner, J.,Tomko, K.,Willis, M.,Kelleher, C.,Cloutier, M.,Husby, E.,Foga, S.,Nakamura, H.,Platson, M.,Wethington, M., Jr.,Williamson, C.,Bauer, G.,Enos, J.,Arnold, G.,Kramer, W.,Becker, P.,Doshi, A.,D'souza, C.,Cummens, P.,Laurier, F. & Bojesen, M. 2018. ArcticDEM. Harvard Dataverse.

Ramsey, B. C. 2009. Bayesian Analysis of Radiocarbon Dates. *Radiocarbon,* 51**,** 337-360.

Rasmussen, S. O.,Abbott, P. M.,Blunier, T.,Bourne, A. J.,Brook, E.,Buchardt, S. L.,Buizert, C.,Chappellaz, J.,Clausen, H. B.,Cook, E.,Dahl-Jensen, D.,Davies, S. M.,Guillevic, M.,Kipfstuhl, S.,Laepple, T.,Seierstad, I. K.,Severinghaus, J. P.,Steffensen, J. P.,Stowasser, C.,Svensson, A.,Vallelonga, P.,Vinther, B. M.,Wilhelms, F. & Winstrup, M. 2013. A first chronology for the North Greenland Eemian Ice Drilling (NEEM) ice core. *Climate of the Past,* 9**,** 2713-2730.

Reimer, J. P.,Bard, E.,Bayliss, A.,Beck, J. W.,Blackwell, P. G.,Ramsey, C. B.,Buck, C. E.,Cheng, H.,Edwards, R. L.,Friedrich, M.,Grootes, P. M.,Guilderson, T. P.,Haflidason, H.,Hajdas, I.,Hatté, C.,Heaton, T. J.,Hoffmann, D. L.,Hogg, A. G.,Hughen, K. A.,Kaiser, K. F.,Kromer, B.,Manning, S. W.,Niu, M.,Reimer, R. W.,Richards, D. A.,Scott, E. M.,Southon, J. R.,Staff, R. A.,Turney, C. S. M. & Van Der Plicht, J. 2013. Intcal13 and Marine13 radiocarbon age calibration curves 0-50,000 years cal BP. *Radiocarbon,* 4**,** 1869-1887.

Stone, J. O. 2000. Air pressure and cosmogenic isotope production. *Journal of Geophysical Research: Solid Earth,* 105**,** 23753-23759.

549 Young, N. E.,Briner, J. P.,Rood, D. H.,Finkel, R. C.,Corbett, L. B. & Bierman, P. R. 2012. Age of
550 the Fjord Stade moraines in the Disko Bugt region, western Greenland, and the 9.3 and
551 8.2 ka cooling events. *Quaternary Science Reviews,* 60**,** 76-90.
552 Young, N. E.,Schaefer, J. M.,Briner, J. P. & Goehring, B. M. 2013. A10Be production-rate
553 calibration for the Arctic. *Journal of Quaternary Science,* 28**,** 515-526.

554
555
556
557
558
559
560
561
562
563
564
565
566
567
568
569
570
571
572
573
574
575

576 *Table 1: Sample collection information, ^{14}C ages and calibrated ages for marine molluscs (Q-S), lake sediment cores (Q) and subfossil*
577 *plants (MC) collected in the Qaanaaq area, northwest Greenland.*

Location	Sample name	Sample material	Latitude *(°N)*	Longitude *(°W)*	Elevation (m a.s.l)	Water depth at core site (m)	Distance from ice margin (m)	Age (^{14}C a BP)	Age (95% range) (cal a BP)	Mean Age (k cal a BP)
West Taserssuit Valley	Q-S1a	Hiatella arctica	77.70266	69.41389	32	-	-	31159±174	34173-34896	34.5±0.4
	Q-S1b	Hiatella arctica	77.70266	69.41389	32	-	-	33599±329	36345-38261	37.3±1.0
	Q-S1c	Hiatella arctica	77.70266	69.41389	32	-	-	35754±285	39030-40469	39.8±0.7
	Q-S2a	Hiatella arctica	77.70308	69.41389	40	-	-	31420±181	34395-35171	34.8±0.4
	Q-S2b	Hiatella arctica	77.70308	69.41389	40	-	-	32770±180	35670-36495	36.1±0.4
	Q-S2c	Hiatella arctica	77.70308	69.41389	40	-	-	31855±145	34805-35564	35.2±0.4
	Q-S3a	Hiatella arctica	77.69444	69.40528	15	-	-	33043±210	35861-36997	36.4±0.6
	Q-S3b	Hiatella arctica	77.69444	69.40528	15	-	-	38440±299	41734-42604	42.2±0.4

	Q-S3c	Hiatella arctica	77.69444	69.40528	15	-	-	26827±115	30288-30893	30.6±0.3
	Q-S4a	Mya truncata	77.68712	69.44944	52	-	-	35253±206	38695-39746	39.2±0.4
	Q-S4b	Mya truncata	77.68712	69.44944	52	-	-	36174±309	39523-41016	40.3±0.7
	Q-S4c	Mya truncata	77.68712	69.44944	52	-	-	32400±203	35255-36216	35.7±0.5
Northwest Taserssuit Valley	Q3	Bulk	77.69757	69.35635	16	10.7	-	6298±67	7018-7415	7.2±0.2
	Q4	Plant macrofossil	77.70728	69.40652	47	11.2	-	7010±48	7726-7945	7.8±0.1
	Q5a	Plant macrofossil	77.70713	69.41987	43	17.2	-	4626±44	5087-5572	5.4±0.2
	Q6	Bulk	77.70066	69.44299	16	0.9	-	1551±40	1357-1533	1.5±0.1
Southeast Taserssuit Valley	Q7	Plant macrofossil	77.68190	69.21202	79	15.1	-	6138±44	6911-7164	7.0±0.1
Northern side of	MC2	Subfossil Plant	77.65178	69.30917	588	-	20-30	1098±28	939-1062	1.0±0.1

Qaanaaq Ice Cap	MC3	Subfossil Plant	77.65178	69.30889	606	-	20-30	1242±30	1074-1269	1.2±0.1
	MC4	Subfossil Plant	77.65181	69.30722	607	-	10	1033±44	800-1058	0.9±0.1
	MC5	Subfossil Plant	77.65181	69.30694	609	-	10	1141±38	967-1175	1.1±0.1
	MC6	Subfossil Plant	77.65225	69.30250	611	-	10	1258±29	1085-1280	1.2±0.1
	MC7	Subfossil Plant	77.65242	69.29833	617	-	10	1167±29	986-1178	1.1±0.1
	MC8	Subfossil Plant	77.65267	69.29528	618	-	10	1173±28	990-1180	1.1±0.1
	MC9	Subfossil Plant	77.65333	69.27222	659	-	0.05	1197±43	988-1260	1.1±0.1
Southern side of Qaanaaq Ice Cap	MC11	Subfossil Plant	77.50128	69.15417	612	-	0.2	3067±32	3181-3364	3.3±0.1
	MC12	Subfossil Plant	77.50092	69.14167	632	-	0.2	3031±39	3080-3357	3.2±0.1
	MC13	Subfossil Plant	77.50064	69.13500	640	-	0.2	2915±31	2964-3159	3.1±0.1

578

579

580

Table 2: Sample collection and ^{10}Be isotopic information for five boulder samples from the Taserssuit Valley (GL1736-GL1740) and three boulder samples from Inglefield Bredning (GL1742-GL1744), northwest Greenland.

Sample Name	Location	Elevation (m a.s.l.)	Latitude (ºN)	Longitude (ºW)	Thickness (cm)	Shielding	Carrier added (g) †	^{10}Be conc. (atoms/g)	^{10}Be unc (atoms/g)	^{10}Be age (ka) ‡	^{10}Be age unc. (ka) §
GL1736	Boulder on moraine	94	77.66400	69.60056	5.4	0.998	0.61788	46062	1915	10357	426
GL1737	Boulder on moraine	94	77.66411	69.58917	5.8	0.998	0.61333	107536	3216	24327	714
GL1738	Boulder on moraine	102	77.66444	69.57972	5.9	0.997	0.61588	68001	2179	15237	480
GL1739	Boulder on moraine	128	77.71889	69.16806	6.3	0.998	0.60909	73626	3309	16073	718
GL1740	Boulder on moraine	119	77.71650	69.18306	6.4	0.998	0.60851	129041	3442	28576	744
GL1742	Boulder on bedrock	74	77.50478	66.67167	3.7	1.000	0.21125	51442	1645	11576	375
GL1743	Boulder on bedrock	74	77.50489	66.66972	6.3	1.000	0.20293	56994	1764	13100	411
GL1744	Boulder on bedrock	74	77.50489	66.66972	6.7	1.000	0.20532	47421	1443	10932	337

†Carrier *Phe1602* (328.2±3.7 μg ^{9}Be/g) was used for preparation of samples GL1736-1740 and carrier *Phe1603* (949.4±6.2 μg ^{9}Be/g) was used for preparation of samples GL1742-GL1744.

585

586 ‡ ^{10}Be ages were calculated using the online exposure age calculator formerly known as the CRONUS-Earth online exposure calculator v.3
587 (Balco et al., 2008), the Baffin Bay/Arctic production rate (Young et al., 2013), and the St scaling scheme (Lal, 1991; Stone, 2000) under
588 standard atmosphere. A rock density of 2.65 g cm^{-3} was used and we assumed zero erosion. Samples were measured using the Beryllium
589 standard 07KNSTD (Nishiizumi et al., 2007). Process blank ^{10}Be/^{9}Be ratios were 8.85332±4.73722E-16 (GL1736-1740) and
590 1.99997±0.458773E-15 (1742-1744).

591 § ^{10}Be age uncertainties are reported as the 1σ internal uncertainty.

592

593

594

595 **Figure captions**

596

597 Fig. 1. Location of the Qaanaaq and Inglefield Bredning study areas. (A) shows the location of the
598 study areas in northwest Greenland. (B) is a close up of the Thule region with places discussed in
599 the text. Black boxes mark the Qaanaaq and Inglefield Bredning study areas. (C) is a close up of the
600 Qaanaaq study area (Landsat-8 satellite imagery). Black boxes show the Taserssuit Valley outlined
601 in Figure 2 and Qaanaaq Ice Cap outlined in Figure 5. D) shows the sample location of sample
602 GL1742-Gl1744 in the Inglefield Bredning study area (Google Earth imagery, 2016) as well as
603 places discussed in the text.

604 Fig. 2. Geomorphological map of the Taserssuit Valley (ArcticDEM hillshade imagery). Sample
605 numbers correspond to lake sediment cores (Q), boulders (GL), reworked molluscs (Q-S) and
606 subfossil plants (MC), collected in the area and discussed in the text. Geomorphological features in
607 the landscape such as moraines, lakes, alluvial fans, ice and deltas are highlighted with different
608 colors.

609

610 Fig. 3. Boulders sampled for ^{10}Be exposure dating in the Taserssuit Valley (A-E) and Inglefield
611 Bredning (F-H), as well as resulting ages. (A-C) shows boulders sampled on the moraine in the far
612 western parts of the Taserssuit Valley whereas (D-E) show boulders collected on the moraine in the
613 far eastern end of the Taserssuit Valley. (F-H) show boulders collected on an island in Inglefield
614 Bredning close to Qeqertat.

615

616 Fig. 4. Summary lithology, colour and X-ray photographs, magnetic susceptibility, titanium, sample
617 location within each core and related calibrated radiocarbon ages for lake cores (Q3-Q7) collected
618 in the Taserssuit Valley.

619

620 Fig. 5. Sampling location for subfossil plants in front of Qaanaaq Ice Cap. (A) shows Qaanaaq Ice
621 Cap (Landsat-8 satellite imagery), with the black boxes outlining the two sampling sites. (B) shows
622 the locations for samples MC2-MC9 on the northern side of Qaanaaq Ice Cap (Landsat-8 satellite
623 imagery) as well as resulting ages (k cal a BP). (C) shows the locations for samples MC11-MC13
624 on the southern side of Qaanaaq Ice Cap (Landsat-8 satellite imagery) as well as resulting ages (k
625 cal a BP). (D) and E) show moss sample MC9 and MC11 respectively.

Fig. 6. Ice and climate fluctuations for north and northwest Greenland during the last 45 ka. (A) Reconstruction of ice-margin fluctuations in the Qaanaaq area and Inglefield Bredning based on ^{14}C ages of reworked molluscs (red), ^{10}Be ages of boulders (blue), ^{14}C ages of sediment cores (green) and ^{14}C ages of mosses (black). (B) Summer temperature reconstruction at 79°N (Larsen et al., 2018; Buizert et al., 2014). (C) Accumulation rate at NEEM (Rasmussen et al., 2013). Vertical light blue bars mark periods when the ice in the study areas was at or behind its present day position.

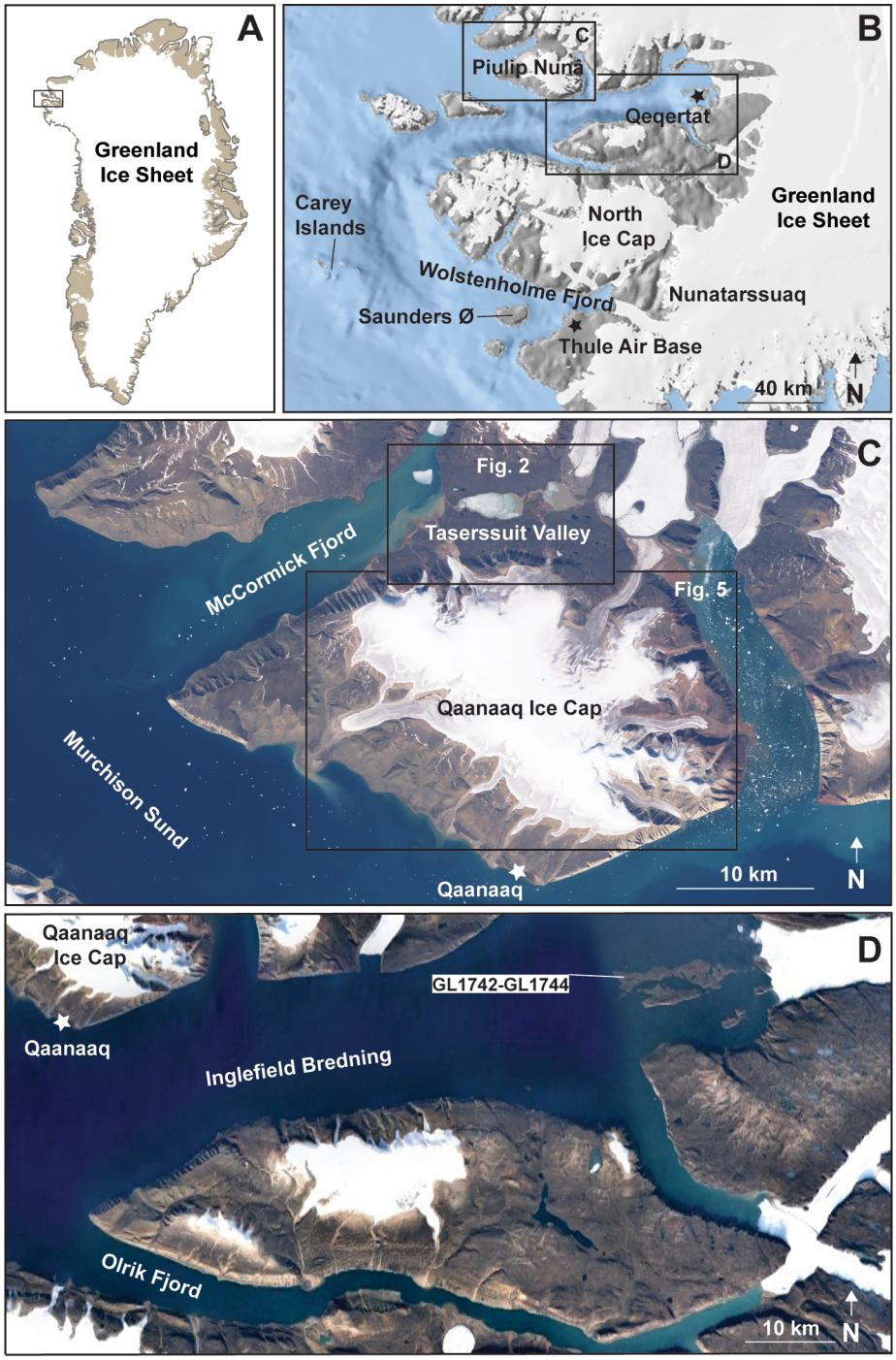
A
Greenland
Ice Sheet
B
C
Piulip Nunâ
Qeqertat
D
Carey
Islands
North
Ice Cap
Greenland
Ice Sheet
Wolstenholme Fjord
Nunatarssuaq
Saunders Ø
Thule Air Base
40 km
N
C
Fig. 2
Taserssuit Valley
McCormick Fjord
Fig. 5
Qaanaaq Ice Cap
Murchison Sund
Qaanaaq
10 km
N
D
Qaanaaq
Ice Cap
GL1742-GL1744
Qaanaaq
Inglefield Bredning
Olrik Fjord
10 km
N

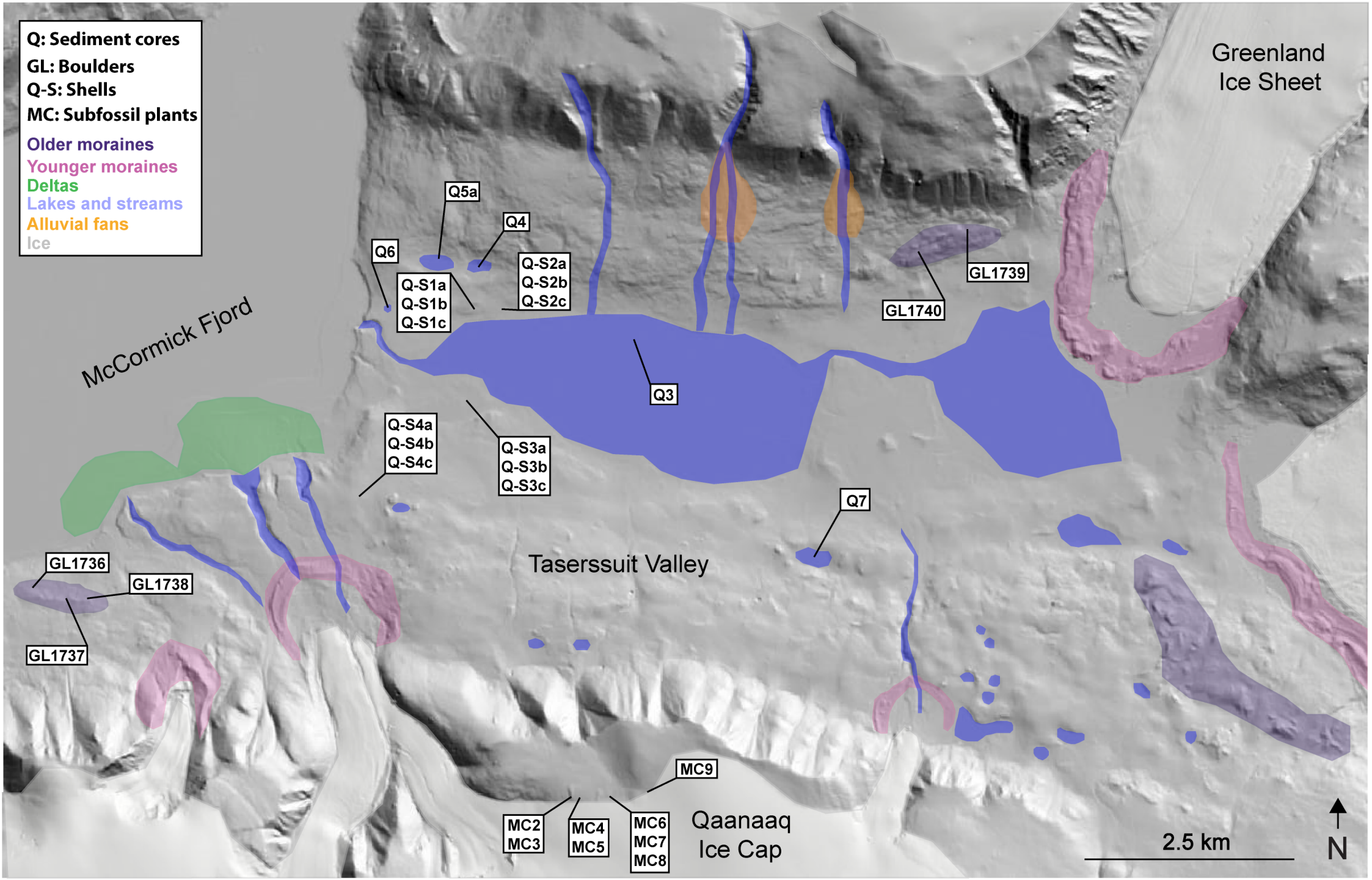
Q: Sediment cores
GL: Boulders
Q-S: Shells
MC: Subfossil plants
Older moraines
Younger moraines
Deltas
Lakes and streams
Alluvial fans
Ice
Greenland Ice Sheet
McCormick Fjord
Taserssuit Valley
Qaanaaq Ice Cap
Q5a
Q4
Q6
Q-S1a
Q-S1b
Q-S1c
Q-S2a
Q-S2b
Q-S2c
GL1739
GL1740
Q3
Q-S4a
Q-S4b
Q-S4c
Q-S3a
Q-S3b
Q-S3c
Q7
GL1736
GL1738
GL1737
MC9
MC2
MC3
MC4
MC5
MC6
MC7
MC8
2.5 km
N


A
GL1736
10.4.±0.4 ka
B
GL1737
24.3±0.7 ka
C
GL1738
15.2±0.5 ka
D
GL1739
16.1±0.7 ka
E
GL1740
28.6±0.7 ka
F
GL1742
11.6±0.4 ka
G
GL1743
13.1±0.4 ka
H
GL1744
10.9±0.3 ka

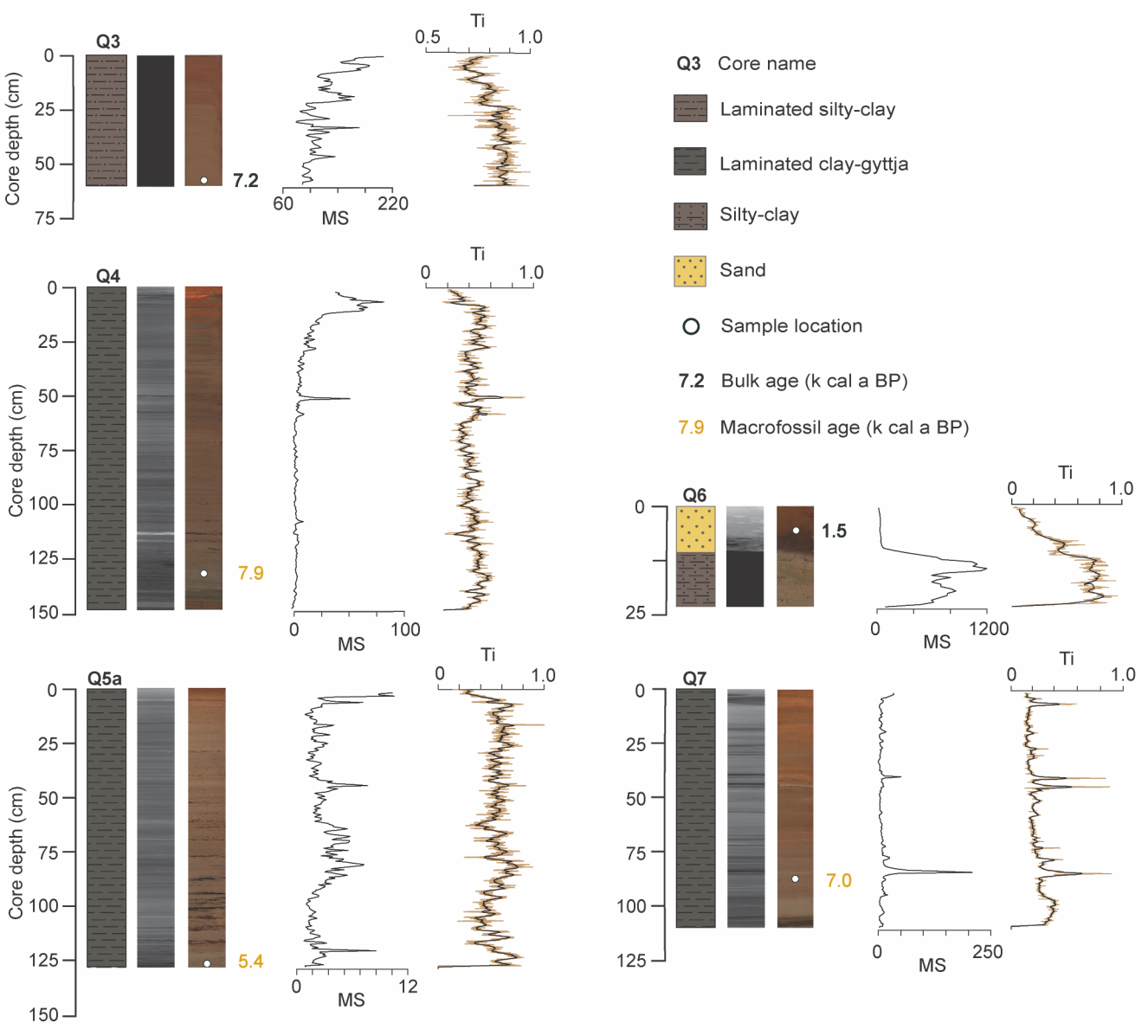
Q3
Core depth (cm)
0
25
50
75
7.2
60
220
MS
Ti
0.5
1.0
Q4
0
25
50
75
100
125
150
7.9
0
100
MS
Ti
0
1.0
Q5a
0
25
50
75
100
125
150
5.4
0
12
MS
Ti
0
1.0
Q3 Core name
Laminated silty-clay
Laminated clay-gyttja
Silty-clay
Sand
Sample location
7.2 Bulk age (k cal a BP)
7.9 Macrofossil age (k cal a BP)
Q6
0
25
1.5
0
1200
MS
Ti
0
1.0
Q7
0
25
50
75
100
125
7.0
0
250
MS
Ti
0
1.0

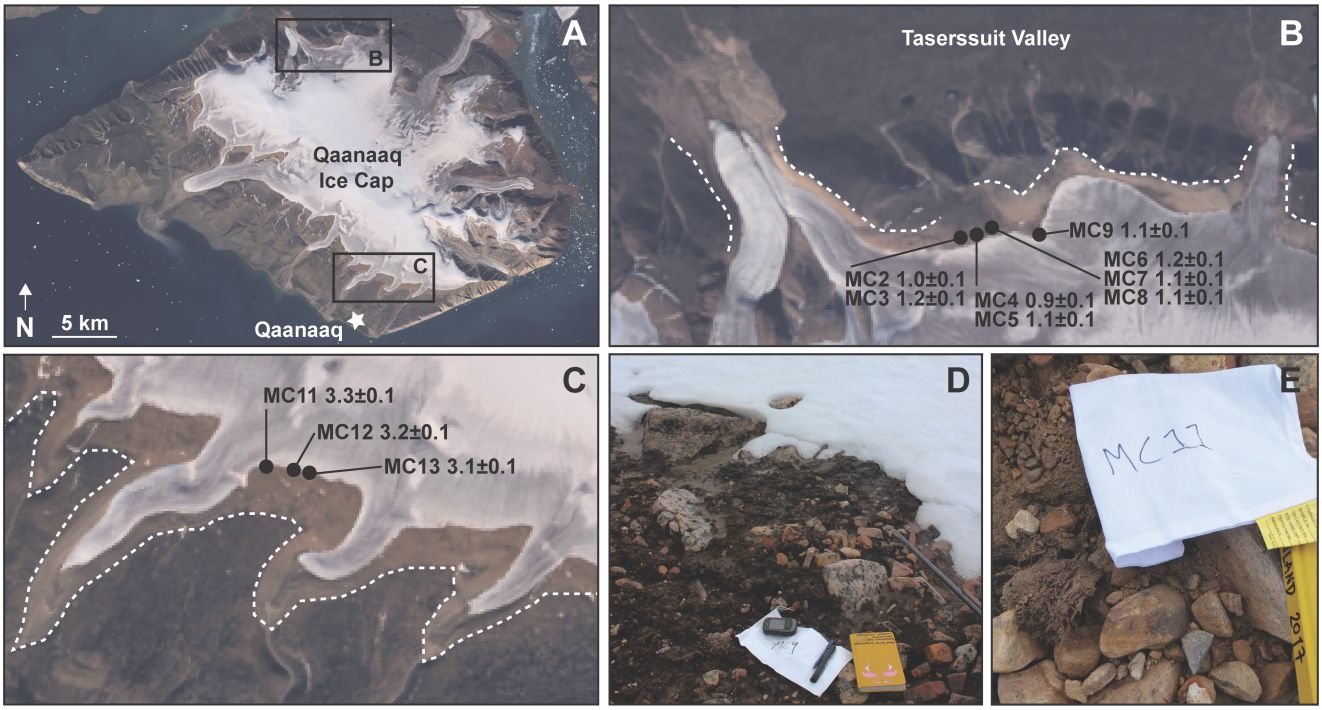
A
B
Qaanaaq
Ice Cap
C
N
5 km
Qaanaaq
Taserssuit Valley
B
MC9 1.1±0.1
MC6 1.2±0.1
MC7 1.1±0.1
MC8 1.1±0.1
MC2 1.0±0.1
MC3 1.2±0.1
MC4 0.9±0.1
MC5 1.1±0.1
C
MC11 3.3±0.1
MC12 3.2±0.1
MC13 3.1±0.1
D
E
MC11

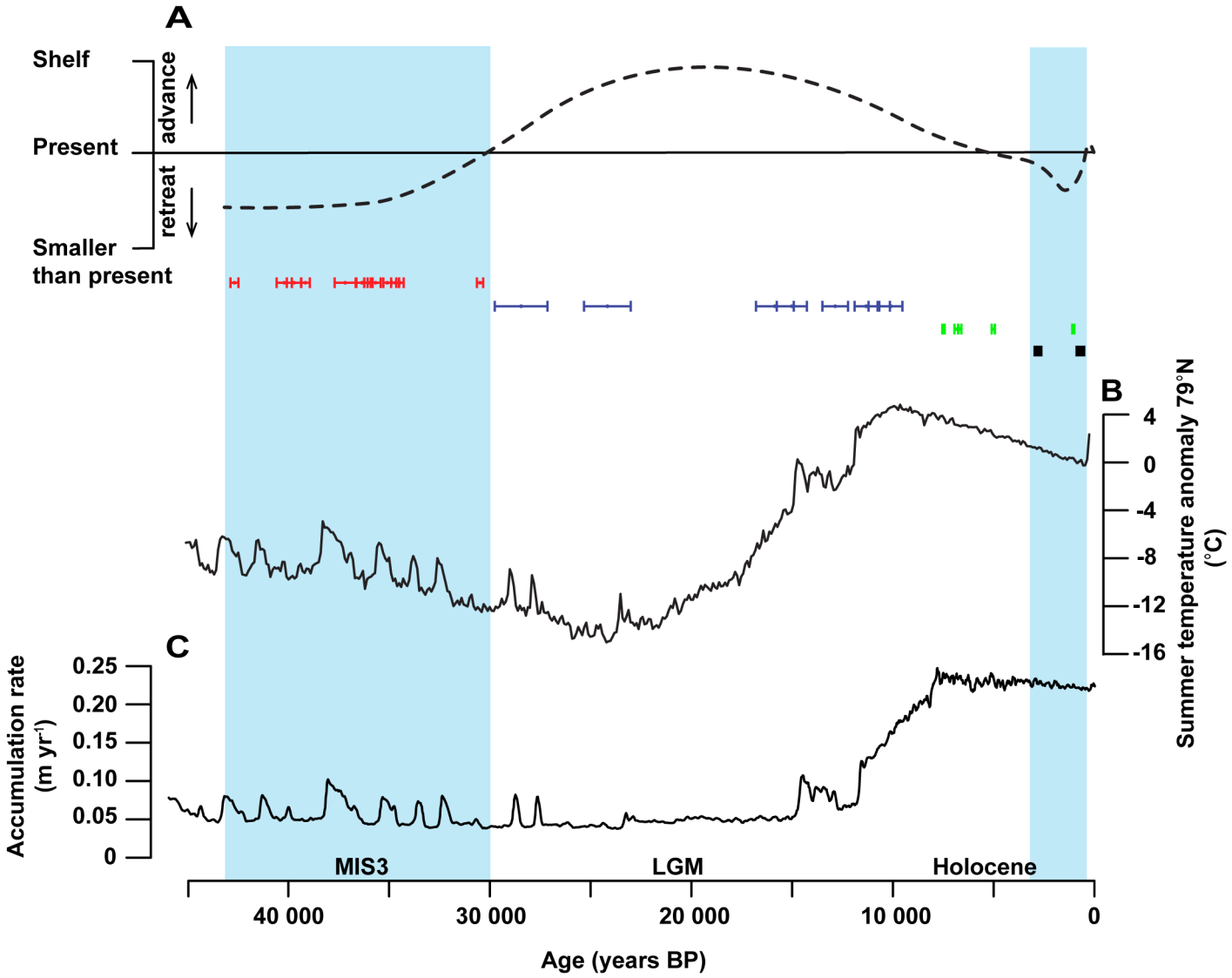
A
Shelf
Present
Smaller
than present
advance
retreat
B
4
0
-4
-8
-12
-16
Summer temperature anomaly 79°N
(°C)
C
Accumulation rate
(m yr⁻¹)
0.25
0.20
0.15
0.10
0.05
0
MIS3
LGM
Holocene
40 000
30 000
20 000
10 000
0
Age (years BP)

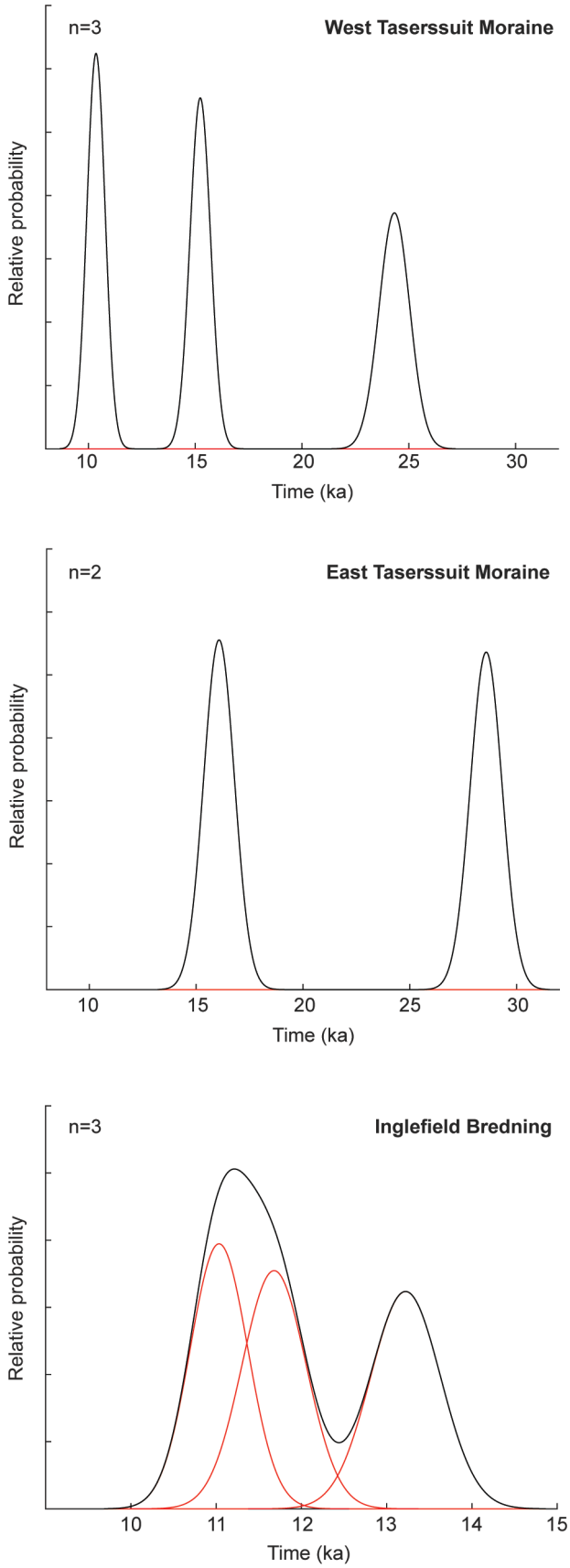
n=3
West Taserssuit Moraine
Relative probability
10
15
20
25
30
Time (ka)
n=2
East Taserssuit Moraine
Relative probability
10
15
20
25
30
Time (ka)
n=3
Inglefield Bredning
Relative probability
10
11
12
13
14
15
Time (ka)

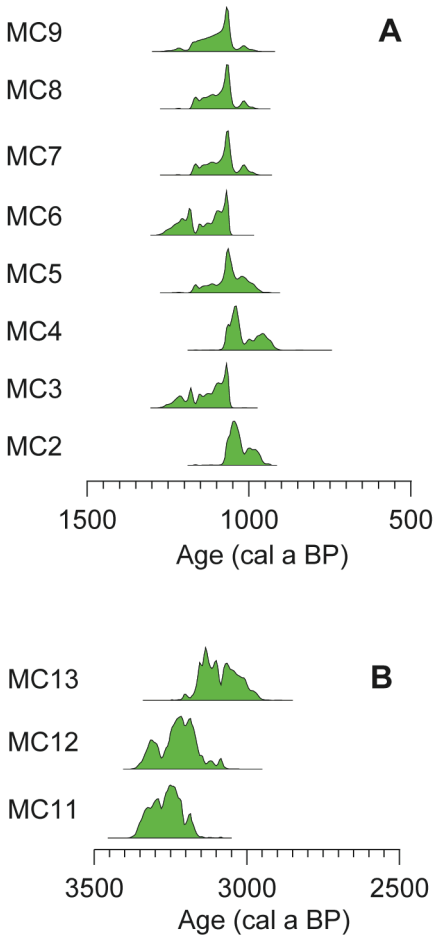
MC9
MC8
MC7
MC6
MC5
MC4
MC3
MC2
A
1500
1000
500
Age (cal a BP)
MC13
MC12
MC11
B
3500
3000
2500
Age (cal a BP)